Quality Control of Scintillation Cameras Using a Minicomputer

Bruce H. Hasegawa, Dennis L. Kirch, Michael T. LeFree, Robert A. Vogel, Peter P. Steele, and William R. Hendee

Veterans Administration Medical Center and the University of Colorado Health Sciences Center, Denver, Colorado

A minicomputer-based technique compiles objective indicators of scintigraphic system performance. The evaluation begins with the acquisition of a single image of an orthogonal hole pattern from which quantitative and regional measurements of point-source sensitivity, spatial resolution, and spatial linearity are derived. Two computer programs offer the user different but complementary features. The first program is the basis of an evaluation performed by a technologist for purposes of quality control. Operator intervention is minimal, and the entire protocol, including data acquisition and processing, can be completed in 20 min. The results are automatically compiled and displayed as graphs showing 100 consecutive sets of daily performance measurements. A second computer program is designed as an interactive diagnostic and research tool to display measurements as histograms and functional images. The operator can use the program to determine the quantitative and spatial characteristics of the system's intrinsic performance measurements made during the quality-control evaluations.

J Nucl Med 22: 1075–1080, 1981

The scintillation camera is the primary imaging device in nuclear medicine and the need to monitor its performance is recognized by investigators, professional societies, hospital accreditation organizations, and governmental agencies (*1–5*). Relatively few procedures use computers for the routine quality control (QC) of scintigraphic systems (*6–9*), although the advantages of computer-based QC measurements have been recognized by several authors (*8,10,11*). Quantitative evaluations of test images would be more objective and precise than visual evaluations. In addition, when a computer is included in the scintigraphic system, the performance can be degraded by the camera's output amplifiers, the cable between the computer and the camera console, the computer interface, or the analog-to-digital converters. Computerized QC measurements derived from digital images include the effects of these camera/computer interface problems.

Received Oct. 14, 1980; revision accepted Aug. 10, 1981.

For reprints contact: Dennis L. Kirch, Div. of Cardiology (111B), Veterans Administration Medical Center, 1055 Clermont St., Denver, CO 80220.

A technique has been developed to evaluate several characteristics from test images acquired with a scintillation camera/computer system. For simplicity, the technique relies on a single image generated with an orthogonal hole pattern (OHP) and a volumetric flood source. A computer program has been written for use as part of a daily QC protocol. This program computes measurements of spatial linearity, spatial resolution, and point-source sensitivity, and displays the results in tabular and graphic form. A second program can be used interactively to quantify the spatial location and magnitude of characteristics revealed during the QC protocol.

MATERIALS

Several commercially available flood tanks and OHPs were tested, but all were manufactured with insufficient stability and precision for quantitative measurements. Therefore, an OHP and flood tank were machined especially to limit the introduction of systematic errors into the results of the evaluation.

The volumetric flood source is a cylindrical tank, 5.3

cm high and 42.5 cm in diameter, with 0.9-cm walls. The tank is milled out of a solid block of plexiglass, with walls of sufficient rigidity to minimize bowing. The tank is filled with a 5- to 10-mCi pertechnetate solution equal in volume to the air volume of the tank. After filling, the sides of the tank are compressed to expel excess air. The flatness of the walls is verified by attempting to slide an 0.2-mm thickness gauge under the edge of a steel ruler placed across the tank. This limits regional variations in source thickness to 1%.

The OHP is a lead plate, 4.76 mm thick and 80 cm in diameter. For large-field cameras, the central region (38.1 cm diameter) of the plate is drilled with a square array of holes, 1.80 mm in diameter, with center-to-center spacings of 19.05 mm. The tolerances on hole spacings and diameters are 0.1 and 0.02 mm, respectively.

METHODS

Image acquisition. The OHP is placed, without a collimator, directly on the detector surface and, after thorough mixing, the flood source is placed directly on the OHP. The detector is tilted to move bubbles in the tank out of the detector's field of view.

The OHP image is acquired as a 16-bit digital matrix with 128 × 128 pixels. To describe the image, the following terminology is introduced. The set of pixels containing counts corresponding to a hole in the OHP is called a "peak." A single pixel containing more counts than its nearest neighbors, located approximately at the center of each peak, is called the "peak maximum" or simply "maximum." To limit statistical uncertainty to 1%, images are acquired so that each peak contains at least 10,000 counts. For a source activity of 10 mCi, acquisition of a 7-million-count image requires ~7 min. Source activities of 30 mCi can be used without measurable changes in image characteristics.

Image processing. The algorithm begins by searching left to right, row by row for peak maxima. A 5 × 5-pixel region of interest is centered over each peak and the counts in this region are summed. After the aggregate count for each peak is obtained, each is expressed as a percent difference from the mean aggregate count and is used as a measurement of the local point-source sensitivity of the detector.

Measurements of spatial linearity and spatial resolution are derived under the assumption that the point-spread function describing the peak is a two-dimensional Gaussian function (*12,13*). After a peak maximum is located, a 3 × 3-pixel region of interest is centered over the peak. Pixels along each column i of the region of interest are summed and a second-order polynomial

$$Z_i = ai^2 + bi + c$$

is fitted to the logarithms of the three resulting sums, Z_i. This defines a set of three simultaneous equations, which can be solved for the polynomial coefficients a, b, and c. The fit is performed with errors introduced by the statistical uncertainty in the pixel values and systematic errors which are discussed in the evaluation section of this paper. The Gaussian mean u_x and standard deviation s_x are computed by

$$u_x = -b/2a,$$

$$s_x = [-1/(2a)]^{1/2}.$$

The full width at half maximum of the peak, $FWHM_x$, is derived from the standard deviation s_x of the Gaussian function to be

$$FWHM_x = (8 \ln 2)^{1/2} s_x$$

and is expressed in mm relative to the detector surface. This is repeated in the orthogonal direction to obtain the mean u_y and resolution ($FWHM_y$) of the peak in the y direction.

Linearity is assessed by comparing the measured peak locations (u_x, u_y) with the ideal locations of the peak (*14*). The ideal locations form a grid of periodically spaced points with spacings equal to the average x and y spacings between adjacent peaks in the OHP image. The center point of the ideal grid is superimposed on the center of the central peak in the OHP image. This definition of linearity provides for comparison of the displacement of a peak relative to every other peak in the OHP image, and not only with those along a particular row or colunm.

Although the OHP has a square array of holes, the average x and average y spacings of the peaks measured from the OHP image differ from one another typically by 1–2%, and the ideal grid is rectangular rather than square. When a square grid of peak locations is used to determine spatial distortion, the difference in x and y

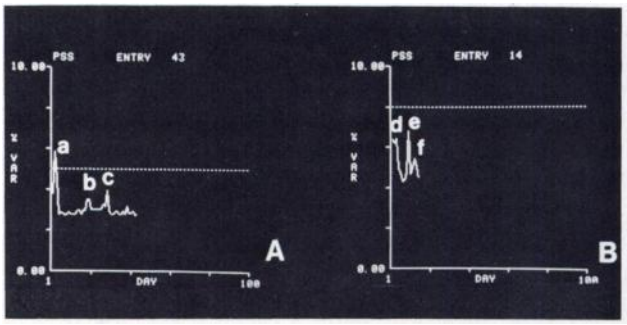

FIG. 1. Graphs of daily point-source sensitivity from two scintillation cameras. Variations of first system (left) occurred when commercial flood tank was replaced with improved model described in MATERIALS section of this paper (point a), and when flood source was mixed inadequately (points b and c). Variations of second system (right) resulted from camera tuning (points d and f) and from inadequate mixing of flood tank (point e). Fluctuations in performance of second system were related to power loss in evenings during hospital construction. Broken line in each daily graph indicates level of "warning threshold" (see text).

spacing ("eccentricity") dominates the computed nonlinearity values and often disguises subtle and localized spatial distortions. Therefore, a rectangular ideal grid is used and the eccentricity of the OHP image is specified as a separate result of the measurements.

Routine quality control. The QC protocol begins with the acquisition of an OHP image using the software supplied by the computer manufacturer.* PROGRAM QC first extracts measurements from the image, then displays the results for the operator. PROGRAM QC requires minimal operator intervention, and both processing and display are performed consistently from day to day so that changes in the measurements can be monitored.

The automatic processing of the OHP image results in 325 regional measurements for x and y spatial linearity, x and y spatial resolution, and point-source sensitivity. For each of these indicators, PROGRAM QC derives a single "composite value" that summarizes the 325 regional measurements. Each composite value is plotted against time, with up to 99 preceding determinations of the same variable. Variations of x and y spatial linearity and of point-source sensitivity are summarized by the standard deviations of the measured values. Spatial resolution in the x and y directions is summarized using the arithmetic means of the measurements. The "daily graphs" (Fig. 1) present performance measurements with the system serving as its own control, since changes in performance are identified from fluctuations in the plotted values.

The daily graphs also contain a "warning threshold" represented as a dashed line. When values exceed this threshold, the operator is warned that further investigations or corrective action may be necessary. Currently, the placement of this threshold is determined subjectively from the measured characteristics over a period of time. In the future it may be possible for the warning threshold to be predetermined by the user or manufacturer on an objective basis, although this is impossible at present.

The output from PROGRAM QC is contained in nine frames, which are photographed onto a single sheet of film. The first frame is a list of system reference information, including the date, source activity level, the hospital name, type of camera, energy window settings, diameter of the crystal, and OHP hole spacing. The second frame tabulates the system sensitivity (detected count rate divided by source activity) and the image eccentricity (average x-peak spacing divided by the average y-peak spacing). Frame 3 is an unprocessed OHP image. Frames 4 through 8 are five daily graphs of the quality-control measurements. Finally, frame 9 lists the averages and standard deviations of the five camera measurements that are derived from the OHP image.

Image processing requires 3 min to perform. The entire QC evaluation, including equipment preparation and cleanup, image acquisition, and processing, can be completed in 20 min or less.

Diagnostic mode. As an adjunct to PROGRAM QC, the second computer program, ACCESS, has been designed as a diagnostic and experimental tool. The operator uses it interactively to display the regional and quantitative information compiled by PROGRAM QC. Two display formats are available. First, a histogram can be generated in which the number of peaks is plotted against the measurements made for those peak locations. A separate histogram can be displayed for each of the five performance variables. Information also can be displayed as functional images in which the regional measurements are coded by the intensity of corresponding areas in the image.

The relationship between functional image intensity and the corresponding regional numerical values can be determined interactively by the operator, who specifies a "window" defining the range of values to be displayed in the functional image. The window-level values can be

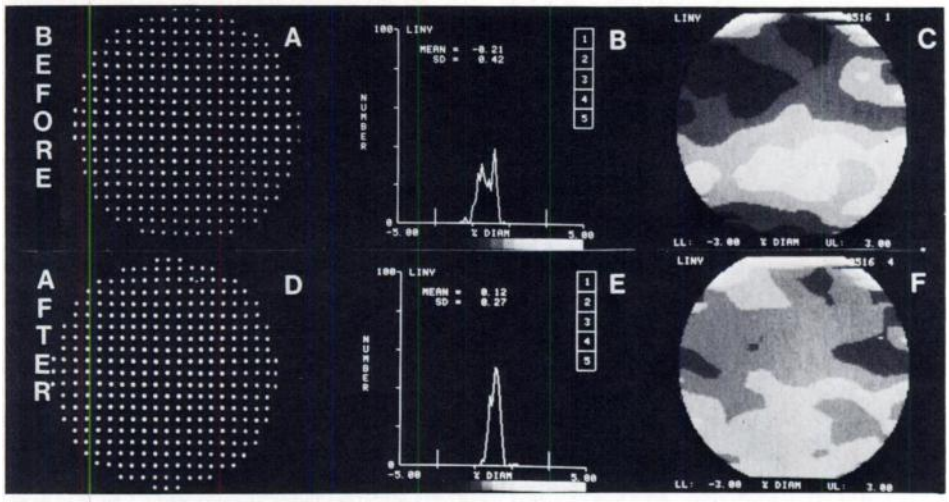

FIG. 2. Images of orthogonal hole pattern (A, D), histograms (B, E), and functional images (C, F) of y spatial linearity before (above) and after (below) camera tuning by a service engineer. Linearity improvement is shown by narrower histogram distribution and more uniform functional image intensity after tuning.

TABLE 1. STATISTICAL ANALYSIS OF 325 PEAK MEASUREMENTS OBTAINED FROM PAIRS OF IMAGES WITH 2 MILLION, 6 MILLION, AND 10 MILLION TOTAL COUNTS

Measurement (units)	Total image counts		
	2 million	6 million	10 million
Point source sensitivity (% variation from mean)	−0.01 ± 1.84*	−0.01 ± 1.08	0.00 ± 0.83
X spatial resolution (mm FWHM)	0.02 ± 0.21	0.00 ± 0.13	0.01 ± 0.10
Y spatial resolution (mm FWHM)	0.00 ± 0.26	0.00 ± 0.15	0.01 ± 0.12
X spatial linearity (% crystal diameter)	−0.01 ± 0.02	−0.01 ± 0.01	0.01 ± 0.01
Y spatial linearity (% crystal diameter)	0.01 ± 0.03	0.02 ± 0.02	−0.01 ± 0.01
X peak coordinate (pixels)	0.01 ± 0.03	−0.01 ± 0.01	0.00 ± 0.01
Y peak coordinate (pixels)	0.01 ± 0.03	0.00 ± 0.02	0.00 ± 0.02

* Values given as mean difference ± one standard deviation.

entered either from the computer keyboard or using a light pen to indicate the desired level on a histogram of measured values displayed on the video monitor. The functional image quantifies both the magnitude and location of measurements with respect to the detector surface. Figure 2 shows OHP images, histograms, and functional images of spatial linearity before and after the camera was tuned by a service engineer.

EVALUATION

Statistical limitations on measurement repeatability. The precision of the method was evaluated by acquiring pairs of OHP images under identical conditions, then comparing the measurements derived from these images. The means and standard deviations of the differences in the paired measurements are shown in Table 1 for image pairs with 2, 6, and 10 million counts. For a 6-million-count image, the uncertainties in paired linearity and resolution measurements are less than 5% of typical manufacturer specifications (approximately 1% of the detector diameter and 4-mm FWHM for linearity and resolution, respectively, in a large-field-of-view camera). The relative point-source sensitivity at a given location on the detector has a statistical uncertainty of ~1% for the 6-million-count image. Currently, OHP images are acquired with at least 7 million counts. Users who require greater precision can acquire images with more counts, with a corresponding increase in acquisition time.

Systematic errors. Inherent in this method are several systematic errors that limit the accuracy of the evaluation and provide errors equal to or greater than the statistical uncertainties described above. These systematic errors are discussed individually.

The finite size of the pixels in the image matrix introduces an error into the computation of the resolution measurements (*15*). The digital sampling of an ideal point-spread function can be modeled by the convolution of a Gaussian function by a rectangular function. This model is used to generate factors, stored in the computer as a look-up table, to correct the computed FWHM values for the effects of digital sampling. The factors depend on both the spatial resolution of the camera and the pixel size in the image matrix. For a 128 × 128 matrix and for an instrument with a 4-mm FWHM, this correction decreases the measured FWHM values by approximately 10%.

The finite size of the holes in the OHP introduces an additional error into the FWHM measurements. The determination of spatial resolution typically assumes that the point source is infinitely small and that a finite source broadens the point-spread response of the detector. Smaller holes are not used in the OHP, since they decrease the sensitivity of the system as well as increase the relative imprecision in hole size. The present hole size increases the FWHM measurements by ~5%. This systematic error is not corrected by the computer algorithm, since other effects, such as statistical uncertainties, angular divergence, and digital sampling, introduce similar or larger errors into the measurements.

To generate the OHP image, a flood source is placed in contact with the OHP. Since the cylindrical holes in the OHP have a length of 4.76 mm and a diameter of 1.8 mm, the photons from the flood source pass through the holes with a maximum angular divergence of 21°. This divergence increases the effective size of the point source created by the hole in the OHP. One can reduce the severity of this problem by using a phantom with smaller hole diameters, although as previously discussed, this

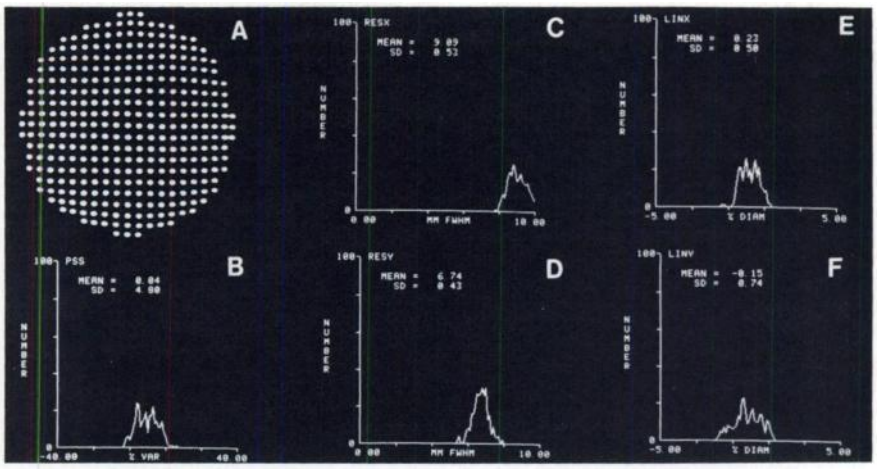

FIG. 3. Histograms of performance measurements on a clinical scintigraphic system. See text for discussion. (A) OHP image; (B) Point-source sensitivity histogram; (C) X spatial resolution histogram; (D) Y spatial resolution histogram; (E) X spatial linearity histogram; (F) Y spatial linearity histogram.

decreases sensitivity and increases relative hole-size variation. Another alternative is to use a distant point source. When this is done, the error in the measured FWHM decreases from about 50% to less than 10%. When accurate resolution measurements are desired, therefore, a distant point source can be used. Unfortunately, the geometrical efficiency of the imaging system may decrease by an order of magnitude with a distant point source. Also, the OHP collimates the photon beam. Since more photons pass through holes directly beneath the point source than through more peripheral holes, an unacceptable regional variation is introduced into the point-source sensitivity measurements. For purposes of quality control, a flood tank must be used to generate the OHP image so that point-source sensitivity and relative spatial resolution can be measured simultaneously.

The present phantom design includes a 3% variation in hole cross-sectional area, which is introduced into the point-source sensitivity measurements. Comparative manual measurements have demonstrated a regional variation of 1% in the sensitivity of a typical well-tuned camera. A sensitivity variation of approximately 3.5% was obtained from the same camera using the computerized OHP technique. A method to reduce or eliminate this systematic error has not been developed. When more accurate quantitative measurements of point-source sensitivity are required, one must rely on manual measurements (*16*).

EXAMPLES

(1) Histograms showing the results of a camera evaluation are given in Fig. 3. The measured spatial resolutions of the camera, not corrected for angular divergence of gamma rays, are 9-mm FWHM in the x direction and 7-mm FWHM in the y direction. This difference in spatial resolution is perceptible by an el-

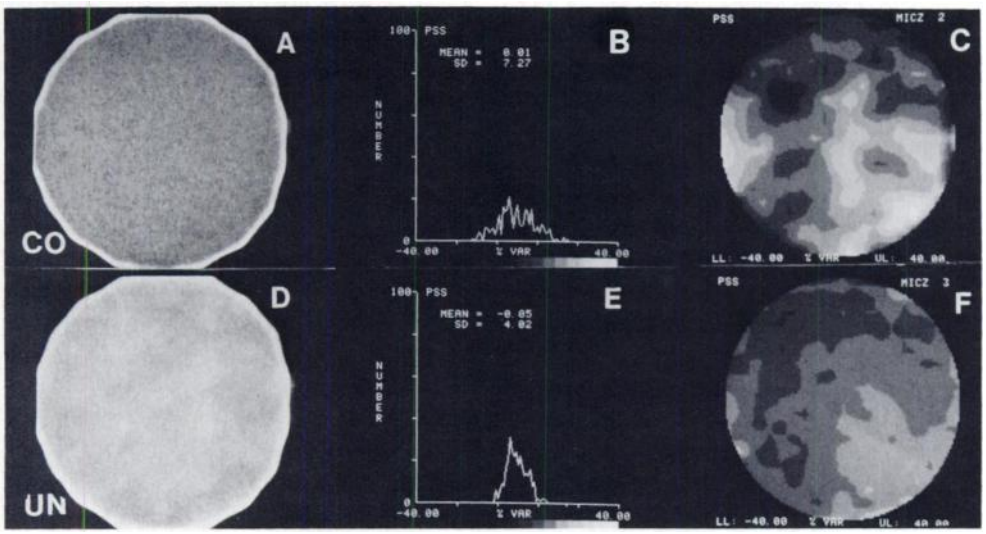

FIG. 4. Flood images (A, D), point-source sensitivity histograms (B, E), and functional images (C, F) show degradation of camera equisensitivity with uniformity correction (top row).

lipticity in the normally circular peaks in the OHP image (Fig. 3A). In addition, the histograms indicate poorer spatial linearity in the y than in the x direction. This difference in spatial linearity is apparently a manifestation of barrelling in the horizontal rows of peaks in the OHP image. Underlying reasons for these linearity and resolution characteristics are unknown at this time.

(2) The effect on point-source sensitivity of uniformity correction was examined by acquiring two OHP images under identical conditions except that one image was obtained with uniformity correction and the other without. Histograms and functional images for point-source sensitivity (Fig. 4) show a degradation in point-source equisensitivity when uniformity correction is used (*17–20*).

DISCUSSION AND SUMMARY

The computerized evaluation described in this report includes tests of spatial linearity, spatial resolution, and point-source sensitivity of the scintillation camera/computer system. Tests of uniformity and low contrast detectability (*21*) are not included but are important components of a complete QC protocol. The computerized evaluation is limited to intrinsic measurements of the scintigraphic system. Tests for uniformity and low contrast detectability are important for the evaluation of display units, multiformat cameras, collimators, and uniformity-correction microprocessors.

However, our early experience indicates that the computerized technique offers several advantages over traditional techniques. Quantitative measurements provide more reliable, objective, and sensitive tests of camera characteristics than analogous subjective evaluations. Characteristics can be compared objectively between different systems and between measurements made on the same system on different days. In addition, the measurements are easily extended to diagnostic and experimental applications. For example, service engineers can examine functional images as a guide for camera adjustment. Since the functional image display can be adapted to show any level of detail, abnormal characteristics are enhanced and identified easily. Finally, since the evaluation is performed on digital images stored in computer memory, the computer is included in the evaluation. This inclusion is essential whenever the computer is to be used in the processing of patient images.

FOOTNOTE

* ADAC Laboratories, Sunnyvale, CA 94086.

ACKNOWLEDGMENTS

The authors are indebted to Charles Gugger, RNMT and Robert Hogue, RNMT for performing clinical trials of the quality-control protocol; to Leonard Shabason, Ph.D. and Victor Spitzer, Ph.D. for technical guidance and criticism; to Martin Kondreck for photography; and to Carol Vandello for preparing the manuscript.

REFERENCES

1. *Nuclear Medicine Services: Accreditation Manual for Hospitals.* Chicago, IL, Joint Commission on Accreditation of Hospitals, 1979
2. BUCHER JE, VAN TUINEN RJ, MOORE MM, et al: Quality assurance in scintillation cameras: an implementation program. *J Nucl Med Tech* 3:87–90, 1975
3. PARAS P: Quality assurance in nuclear medicine. In *Medical Radionuclide Imaging.* IAEA, Vienna, 1977, Vol. 1, pp 3–41
4. *Workshop Manual for Quality Control of Scintillation Cameras in Nuclear Medicine.* Bureau of Radiological Health, FDA 76-8039, 1976
5. *Recommendations for Quality Assurance of Nuclear Medicine Instruments.* American College of Radiology, Committee of Physics, August 1979
6. KEYES JW, GAZELLA GR, STRANGE DR: Image analysis by on-line minicomputer for improved camera quality control. *J Nucl Med* 13:525–527, 1972
7. AYYANGAR K, PATEL J, PARK CH: Quality control of gamma cameras using computer. *Med Phys* 6:335, 1979 (abst)
8. HUTTON BF, CORMACK J: Computer assisted quality control of gamma cameras. *Aust NZ J Med* 9:624, 1979 (abst)
9. *Operating Manual for the Modumed System.* Ann Arbor, MI, Medical Data Systems, 1976
10. BROOKEMAN VA: Computer and quality control in nuclear medicine. *Semin Nucl Med* 8:113–124, 1978
11. WEGST AV, RHODES BA: Where are we going in quality control testing? In *Quality Control in Nuclear Medicine.* B. A. Rhodes, Ed. St. Louis, The C. V. Mosby Company, 1977, pp 368–372
12. BROWNELL GL: Spatial resolution. In *Fundamental Problems in Scanning.* A. Gottschalk, R. N. Beck, Eds. Springfield, Charles C. Thomas, 1968, pp 40–49
13. BUDINGER TF: Instrumentation trends in nuclear medicine. *Semin Nucl Med* 7:285–297, 1977
14. MUEHLLEHNER G: *Radiation Imaging Device.* U.S. Patent 3,745,345, July 10, 1973
15. BROWN DW, KIRCH DL, TROW RS, et al: Quantification of the radionuclide image. *Semin Nucl Med* 3:311–325, 1973
16. *Performance Measurements of Scintillation Cameras.* Washington, DC, National Electrical Manufacturers Association (NEMA), 1980, Standards Publication No. NU 1-1980
17. TODD-POKROPEK AE, ERBSMAN F, SOUSSALINE F: The nonuniformity of imaging devices and its impact on quantitative studies. *Medical Radionuclide Imaging.* Vienna, IAEA, 1977, Vol. 1, pp 67–84
18. PADIKAL TN, ASHARE AB, KEREIAKES JG: Field flood uniformity correction: benefits or pitfalls? *J Nucl Med* 17: 653–656, 1976
19. KNOLL GF, BENNETT MC, STRANGE DR: Real time correction of radioisotope camera signals for nonuniformity and nonlinearity. *J Nucl Med* 19:746, 1980 (abst)
20. KIRCH DL, SHABASON L, LEFREE MT, et al: Anger camera nonuniformity—the source and the cure. *J Nucl Med* 19:712, 1978 (abst)
21. LEWELLEN KT, GRAHAM MM: A low-contrast phantom for daily quality control. *J Nucl Med* 22:279–282, 1981